AJNR

Plasticity of the Human Motor Cortex in Patients with Arteriovenous Malformations: A Functional MR Imaging Study

Hatem Alkadhi, Spyros S. Kollias, Gérard R. Crelier, Xavier Golay, Marie-Claude Hepp-Reymond and Anton Valavanis

AJNR Am J Neuroradiol 2000, 21 (8) 1423-1433
http://www.ajnr.org/content/21/8/1423

AJNR Am J Neuroradiol 21:1423–1433, September 2000

Plasticity of the Human Motor Cortex in Patients with Arteriovenous Malformations: A Functional MR Imaging Study

Hatem Alkadhi, Spyros S. Kollias, Gérard R. Crelier, Xavier Golay, Marie-Claude Hepp-Reymond, and Anton Valavanis

BACKGROUND AND PURPOSE: **The capacity of the human brain to recover from damage has been explained on the basis of plasticity, according to which remaining areas assume functions that would normally have been performed by the damaged brain. Patients with cerebral arteriovenous malformations (AVMs) involving primary motor areas may present without significant neurologic deficits. We used functional MR imaging to investigate the organization of cortical motor areas in patients with AVMs.**

METHODS: **Cortical motor hand and foot representations were mapped in nine right-handed patients harboring AVMs occupying the hand (n = 6) or foot (n = 3) region of the primary motor cortex (M1). None of the patients exhibited motor deficits. Simple movements of the hand and foot were performed. In eight patients, both right and left extremities were tested; in one patient, only the hand contralateral to the AVM was examined. Localization of activation in the affected hemisphere was compared with that in the unaffected hemisphere and evaluated with respect to the normal M1 somatotopic organization shown in earlier functional MR imaging investigations.**

RESULTS: **Cortical activation showed three patterns: 1) functional displacement within the affected M1 independent of the structural distortion induced by the AVM (n = 4), 2) presence of activation within the unaffected M1 ipsilateral to the moving extremity without activation in the affected M1 (n = 3), and 3) prominent activation in nonprimary motor areas without activation in either the affected or unaffected M1 (n = 2).**

CONCLUSION: **Preliminary evidence suggests that brain AVMs lead to reorganization within the somatotopic representation in M1 and to occasional abnormal expansion into nonprimary motor areas.**

Cerebral arteriovenous malformations (AVMs) are generally considered to be inborn errors of vascular morphogenesis caused by a defect or malfunction of the embryonic capillary maturation process (1–4). However, there is increasing evidence that the majority of cerebral AVMs develop postnatally and represent various types of endothelial cell dysfunction (4, 5). Brain AVMs exhibit wide variability in size, hemodynamic features, and vascular composition so that accurate determination of the natural history of an individual case is difficult and may even be impossible (4). The most common initial manifestation, which is estimated to occur at a rate of more than 50%, is hemorrhage. Focal neurologic symptoms without previous hemorrhage occur only in about 8% of patients and may be caused by several factors, including steal effect, decreased perfusion due to arterial stenoses, venous hypertension, and mass effect resulting from compression of the brain parenchyma by venous varices (2–4).

Conventional MR imaging, which provides precise topographic localization of brain AVMs, is an essential tool for therapeutic planning (3, 4). However, the anatomic location alone does not give any information on possible functional reorganization. Thus, in regions adjacent to vascular malformations, brain functions have previously been mapped using a variety of preoperative and intraoperative techniques. Functional MR imaging has proved to be an extremely valid preoperative tool that closely agrees

Received September 1, 1999; accepted after revision March 1, 2000.

From the Institute of Neuroradiology, University Hospital of Zurich, Switzerland (H.A., S.S.K., G.R.C., X.G., A.V.), and the Institute of Neuroinformatics, University Zurich-Irchel, Switzerland (M-C.H-R.).

Supported by the Swiss National Research Program NRP 38 # 4038-052837/1.

Address reprint requests to Spyros S. Kollias, MD, Institute of Neuroradiology, University Hospital of Zurich, Switzerland, Frauenklinikstr. 10, CH-8091, Zurich, Switzerland.

with the results from intraoperative cortical stimulation (6, 7). Several studies and case reports with AVMs involving such brain areas as the sensorimotor, language, and visual cortex, have confirmed the feasibility of functional MR imaging studies in vascular malformations of the brain (6–14). The technique has proved to be of benefit in planning treatment, particularly in patients undergoing surgery. Although in patients undergoing endovascular treatment the functional status of the brain may be tested by local injection of anesthetics, functional brain MR imaging provides the opportunity to noninvasively address important physiological questions related to cortical reorganization by providing information concerning extensive brain territories. However, to date, no systematic studies have attempted to determine the impact of cerebral AVMs on the reorganization of motor function.

The aim of this study was to use functional MR imaging to map cortical organization in patients with brain AVMs directly involving the hand or foot region of the primary motor cortex (M1) and to test the hypothesis according to which brain AVMs would lead to reorganization, thus revealing the large-scale plasticity of the human brain.

Methods

Subjects

Nine right-handed patients (three women and six men; mean age, 34 ± 9 years) harboring MR and angiographically documented AVMs were included in this prospective study. The AVMs were located primarily in the rolandic region, including the central sulcus, the precentral gyrus, or the paracentral lobule, and occupied the somatotopically expected M1 hand or foot representation (15, 16). The subjects were referred for endovascular treatment (n = 5) or for follow-up studies after partial embolization (n = 4). With the exception of patients 3 and 6, who both had MR imaging findings of perinidal gliosis, no patient had MR evidence of additional, associated lesions; and no patient had evidence of hemorrhage. Patients 2 and 9 had experienced a transitory episode of mild hemiparesis that had resolved completely within days. These patients were included in the study owing to their normal neurologic status at the time of functional MR imaging and because of the lack of associated lesions on structural MR images. At the time of functional MR imaging, no patient showed any motor deficit at neurologic examination. All experiments were conducted with the oral consent of the patients.

Functional MR Imaging Data Acquisition

Morphologic and functional MR imaging experiments were performed during the same imaging session with a 1.5-T whole-body MR imaging system with echo-planar capabilities and a standard whole-head transmit-receive coil. Morphologic imaging included acquisition of an axial T2-weighted double-echo fast spin-echo sequence (TR/TE/excitations = 3500/12,102/2, section thickness = 4 mm, gap = 1.3 mm); coronal and sagittal T1-weighted spin-echo sequences (500/10/4, section thickness = 4 mm, gap = 1.3 mm); a 3D time-of-flight sequence (section thickness = 0.6 mm, matrix = 512 × 256); and a 3D phase-contrast MR angiographic sequence (section thickness = 1.2 mm, matrix = 256 × 160). Blood oxygen level–dependent (BOLD) functional MR imaging studies (single-shot echo-planar imaging: 3000/40, flip angle = 60°, voxel size = 2.5 × 2.5 × 5 mm) covered the primary and nonprimary motor areas with eight (n = 6) or 11 (n = 3) sections. To keep imaging time as short as possible, 40 images per section were acquired during five alternating periods of rest-task performance (5, 10, 10, 10, and 5 phases, respectively). The rest period in between tasks was 30 seconds. Simulations with computer-generated signals had confirmed that with 40 measured time points, 98.5% of correlated pixels with a signal change of 1% are detected. Pixels with a signal change above 1% were detected in 100% of simulations. Keeping functional MR imaging experiments short (2 minutes each) allowed us to stay within a total imaging time of 50 minutes, which was well tolerated by all patients.

To map the motor cortical hand and foot representation, the patients were asked to perform simple, self-paced movements at a constant rhythm of approximately one cycle per second. They had to open and close either the left (n = 8) or right (n = 8) hand and/or to make a flexion-extension movement of the left (n = 4) or right (n = 4) foot. The motor tasks were explained to the subjects and practiced before the functional MR imaging data acquisition. During the experiments, patients had their eyes closed; foam cushions and straps were used to immobilize their head.

Functional MR Imaging Data Analysis

To minimize artifacts due to residual head motion, the functional images were realigned for each experiment using an automatic image registration algorithm (17). To compute activation maps, voxels activated during the task conditions were identified by calculating nonparametric Spearman rank order correlation coefficients (18) between the time series of pixel intensities and an idealized response function. Transformation to a Student's *t*-test were made (19) in which only pixels with statistically significant correlation ($P < .005$) were considered as activated areas. The data were postprocessed with a time shift of 6 seconds (two TRs) between stimulus onset and signal intensity change. To account for the fact that the hemodynamics adjacent to AVMs are likely to differ from those in healthy tissue, we reprocessed all data with three different signal models: a boxcar function with 1) a one-TR and 2) a three-TR delay, and 3) a trapezoidal function with a one-TR delay and a rise time of two TRs (see appendix). Additionally, we visually inspected the plotted time courses of voxels in the regions affected by the AVMs.

The activation maps were overlaid onto anatomic high-resolution 3D whole-brain images (3D spoiled gradient-echo sequence: 50/9, flip angle = 45°, matrix = 256 × 192, section thickness = 2 mm). Overlaying the functional MR imaging data on the 3D volume in which the feeding and draining vessels were readily distinguished prevented the possibility of including false-positive areas of activation, particularly those coming from multiple draining veins. The location of the activation was analyzed with respect to the nidus and to feeding and draining vessels as defined by digital subtraction angiography in combination with MR imaging and MR angiography. Activation within the affected hemisphere was compared with that in the unaffected hemisphere and with somatotopic maps recently obtained with functional MR imaging (15, 16).

Results

Structural imaging and angiography revealed nine AVMs with the nidus involving the expected primary motor hand (n = 6) or foot (n = 3) representation (15, 16). Patient data, AVM characteristics and location, and clinical presentation are summarized in Table 1.

Functional MR images showed signal intensity changes in the range of 1% to 4% between rest and activation conditions for all patients. This gave an

TABLE 1: Characteristics of patients and arteriovenous malformations (AVMs)

Patient No.	Sex/Age (y)	Anatomic Location of AVMS	Characteristics of AVMs*	Clinical Presentation
1	M/28	L precentral gyrus, central sulcus	Plexiform, sulcal/gyral paraventricular extension	Focal seizures, R hand
2	M/45	R precentral gyrus, central sulcus	Mixed fistulous and plexiform, sulcal/gyral	Transitory L hemiparesis
3	F/21	R precentral gyrus	Plexiform, gyral, paraventricular extension	Headache, nausea
4	M/42	L precentral gyrus, central sulcus, and precentral sulcus	Plexiform, sulcal, paraventricular extension	Grand mal seizure
5	M/28	L precentral gyrus, central sulcus	Plexiform, sulcal/gyral	Focal seizures, R hand
6	F/22	L central sulcus	Plexiform, sulcal, subcortical extension	Focal seizures, R hand
7	M/38	R paracentral lobule and precuneus	Mixed fistulous and plexiform, sulcal/gyral	Headache
8	F/40	R paracentral lobule	Plexiform, gyral	Transitory numbness L foot
9	M/35	L paracentral lobule	Plexiform, sulcal/gyral	Transitory R hemiparesis

* According to topographic and angioarchitectural classification system of Valavanis (3).

TABLE 2: Activated primary and nonprimary motor areas during contralesional limb movements*

Patient	Ipsilesional Hemisphere Contralateral to the Movement					Contralesional Hemisphere Ipsilateral to the Movement				
No.	M1	SMA	PMd	PA	CMA	M1	SMA	PMd	PA	CMA
1	+	+	−	+	−	−	+	−	+	−
2	+	−	+	+	+	+	+	+	+	+
3	+	+	−	+	−	+	+	+	+	−
4	+	+	+	+	+	−	+	+	+	+
5	−	+	+	+	+	+	+	+	+	+
6	−	+	−	+	+	−	+	+	−	−
7	−	−	−	+	−	+	+	+	+	+
8	−	+	+	+	−	+	+	+	+	+
9	−	−	+	+	+	−	+	+	+	+

* Hand movements in patients 1–6, foot movements in patients 7–9.

Note.—+ indicates presence and − indicates absence of activation; M1, primary motor cortex; SMA, supplementary motor areas; PMd, dorsal premotor areas; PA, parietal areas; CMA, cingulate motor areas.

additional assurance that the functional MR imaging signal had a significant parenchymal contribution and was not dominated by signal from draining veins, in which the expected changes are in the range of 5% to 10%.

In all reprocessed experiments with different time models, the resulting activation maps showed no additional regions of activation either in the primary motor cortex or in the regions affected by the AVMs beyond those seen at postprocessing with a two-TR delay. Additionally, visual inspection of the plotted time courses of voxels in the regions affected by the AVMs revealed no relationship of any kind with the movement paradigm. We thus had strong evidence that the absence of detected activation in any brain area was not the result of a false estimation of the hemodynamic delay.

Significant activation did not lie within the nidus of an AVM or within feeding or proximal draining vessels in any of the experiments. No activation pattern could be related to the size or type (gyral or sulcal) of the individual AVMs.

Activation sites varied among subjects. Activation could be found in the primary motor area (M1) within the central sulcus, including the posterior bank of the precentral and the anterior bank of the postcentral gyrus, as well as in the paracentral lobule. Activation could also be seen in the supplementary motor area (SMA) within the superior frontal gyrus, bordered posteriorly by the paracentral sulcus; in the dorsal premotor areas along the precentral sulcus and its junction with the superior frontal sulcus; in the parietal areas along the intraparietal sulcus, involving the adjacent superior and inferior parietal lobule; and in presumably the cingulate motor areas (CMA) within the cingulate sulcus or gyrus. Table 2 presents a detailed analysis of all activated primary and nonprimary motor areas in both hemispheres during contralesional limb movements.

In six patients (subjects 1–6) with AVMs involving the somatotopically expected M1 hand area, four showed functional displacement within the affected M1 contralateral to the moving limb. Patients 2 and 3 showed additional activation in the ipsilateral M1. Compared with the unaffected hemisphere and with existing somatotopic maps, patients 1 and 2 had a displaced M1 representation

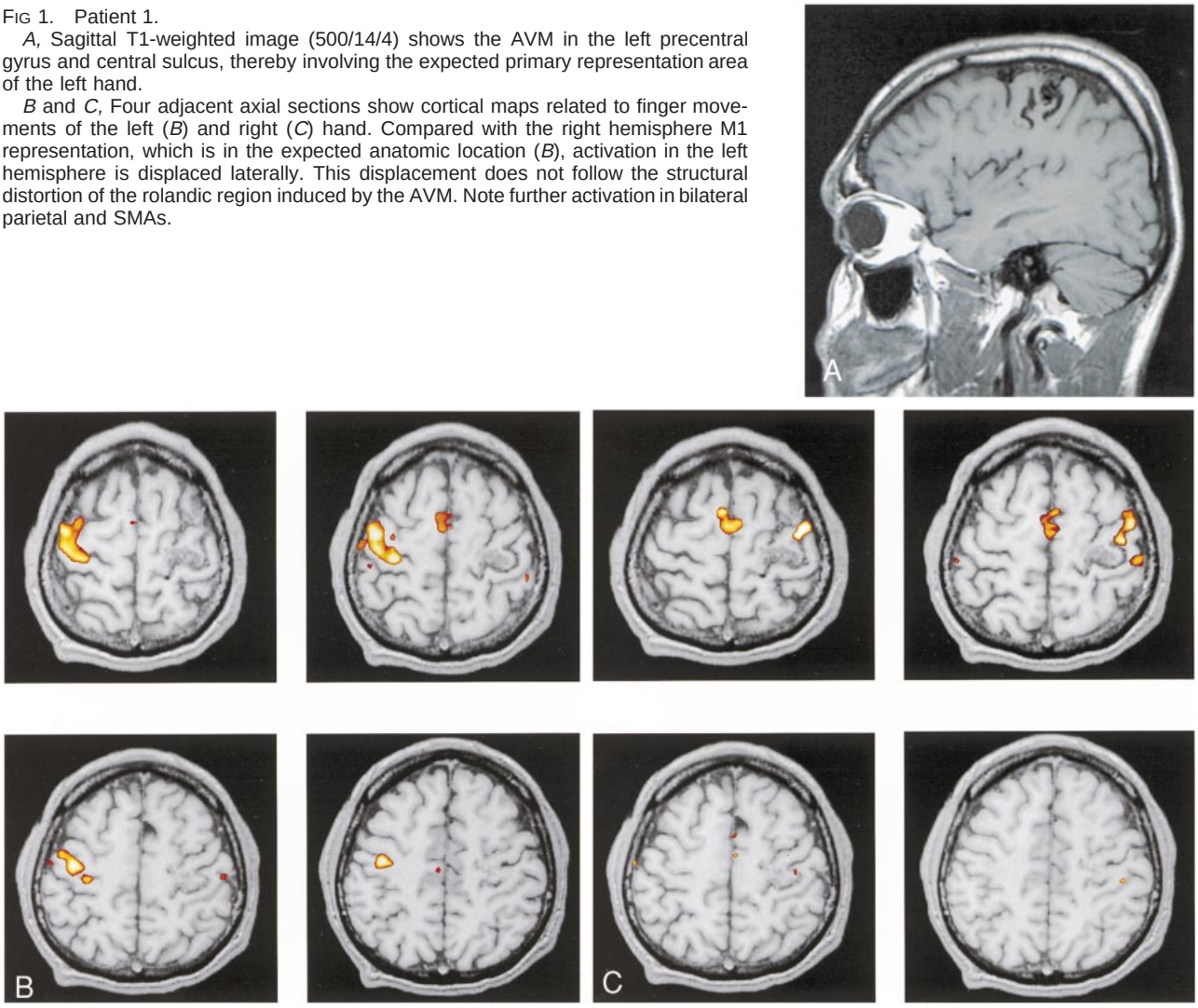

FIG 1. Patient 1.

A, Sagittal T1-weighted image (500/14/4) shows the AVM in the left precentral gyrus and central sulcus, thereby involving the expected primary representation area of the left hand.

B and *C,* Four adjacent axial sections show cortical maps related to finger movements of the left (*B*) and right (*C*) hand. Compared with the right hemisphere M1 representation, which is in the expected anatomic location (*B*), activation in the left hemisphere is displaced laterally. This displacement does not follow the structural distortion of the rolandic region induced by the AVM. Note further activation in bilateral parietal and SMAs.

of the contralateral hand within the precentral gyrus laterally. This is obvious in Figure 1, which displays the representative functional MR imaging sections in patient 1. Compared with the unaffected right side (Fig 1B), M1 activation in the affected hemisphere was clearly displaced laterally (Fig 1C). Patients 3 and 4 had displacement of the M1 hand representation within the precentral gyrus medially, as shown for patient 3 in Figure 2. In this patient, perinidal gliosis was present in the lateral aspect of the precentral gyrus. Activation within the affected right hemisphere was represented by functional displacement medially, with additional signal seen in the ipsilateral M1 (Fig 2C). In all four subjects, the altered maps did not follow the structural distortion of the central region induced by the AVM. Functional MR imaging during right-hand movements in patient 5 showed absent contralateral but present ipsilateral M1 activation in the area of the precentral knob. Patient 6, who presented with focal seizures of the right hand, had an AVM exactly adjacent to the expected M1 hand representation within the left central sulcus. T2-weighted images showed perinidal gliosis in the parenchyma of the postcentral gyrus posterior to the nidus. Figure 3A shows the close relationship of the AVM to the left precentral knob. Two different functional MR imaging sessions repeated within 4 months revealed an absence of M1 activation bilaterally during right-hand movements but prominent bilateral nonprimary motor activation, particularly in the SMA (Fig 3C).

In three patients (subjects 7, 8, and 9) with AVMs involving the somatotopically expected M1 foot representation, two (subjects 7 and 8) showed significant activity in M1 ipsilateral to the moving foot but not contralaterally. In patient 7, an extensive AVM involving the expected right-sided M1 foot representation is shown in Figure 4A. Activation is seen in the ipsilateral M1, SMA, and CMA and in bilateral dorsal premotor and parietal areas (Fig 4C). Patient 9, who had suffered from a transitory and completely regressive right-sided hemiparesis, had a left-sided AVM in the precentral

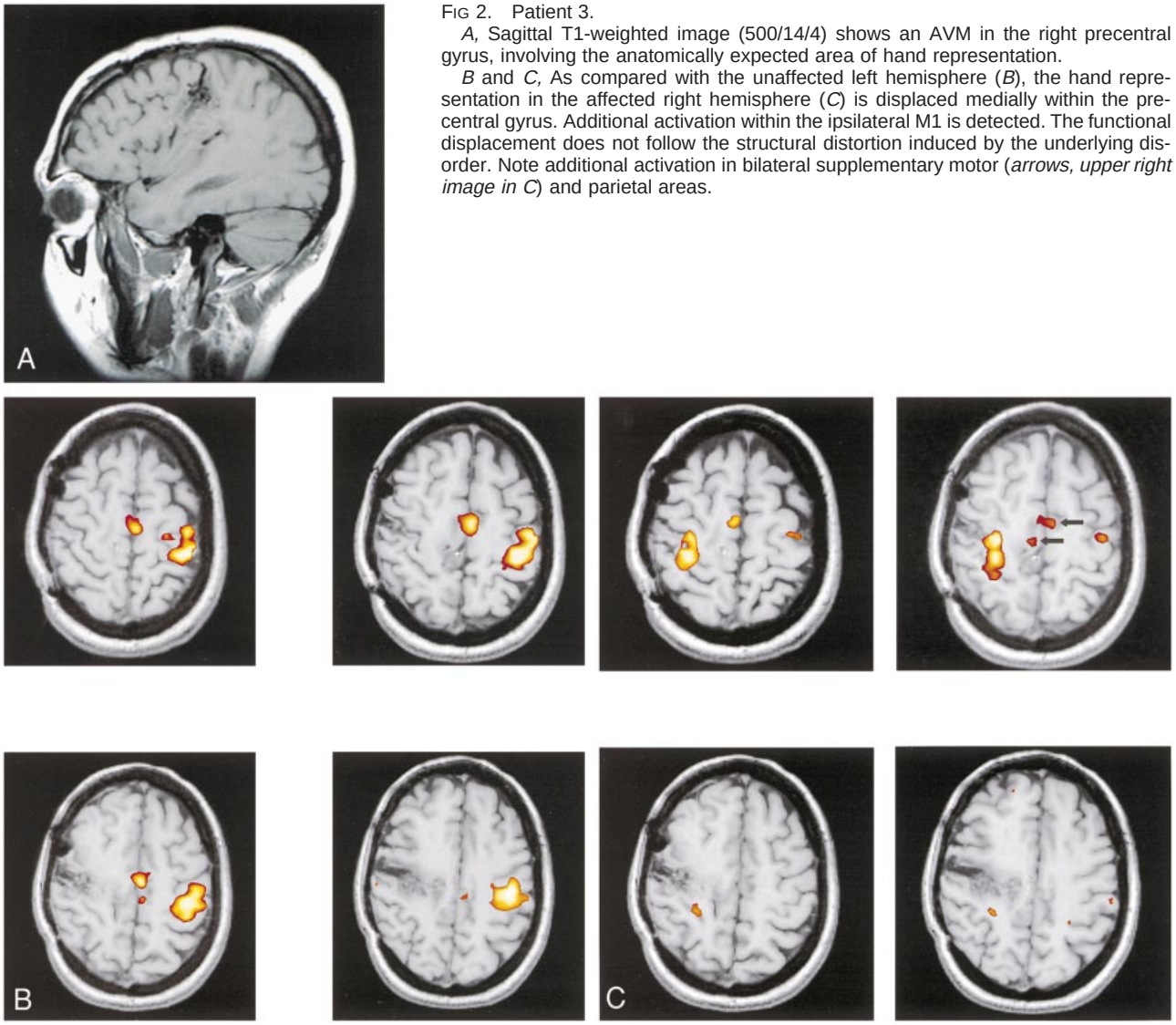

FIG 2. Patient 3.

A, Sagittal T1-weighted image (500/14/4) shows an AVM in the right precentral gyrus, involving the anatomically expected area of hand representation.

B and *C,* As compared with the unaffected left hemisphere (*B*), the hand representation in the affected right hemisphere (*C*) is displaced medially within the precentral gyrus. Additional activation within the ipsilateral M1 is detected. The functional displacement does not follow the structural distortion induced by the underlying disorder. Note additional activation in bilateral supplementary motor (*arrows, upper right image in C*) and parietal areas.

part of the paracentral lobule. Movements of the right foot elicited prominent activation of the dorsal premotor and parietal areas and the CMA bilaterally as well as ipsilateral SMA activation without any activation in M1.

In the experiments performed to obtain an internal control, either by moving the extremity contralateral to the unaffected hemisphere (Figs 1B and 2B) or the limb whose M1 representation was outside the nidus (Figs 3B and 4B), the expected signal in the contralateral M1 was always present.

Cortical activation can be categorized into three patterns: 1) functional displacement within the affected M1 independent of the structural distortion induced by the AVM (patients 1–4); 2) presence of activation within the unaffected M1 ipsilateral to the moving extremity without activation in the affected hemisphere (patients 5, 7, and 8); and 3) prominent activation in nonprimary motor areas without activation in either the affected or the unaffected M1 (subjects 6 and 9).

Discussion

Our results indicate that brain AVMs involving the primary motor hand and foot representations lead to reorganization within the somatotopic representation in M1 contralaterally, with occasional abnormal expansion to supplementary motor, premotor, cingulate, and parietal areas and to the ipsilateral M1. Although previous reports (7, 8, 11–14) corroborate our results of aberrant cortical representation, this is the first study in which the patient selection criteria were strictly limited to AVMs involving precisely the primary motor hand and foot representation and only to patients without motor deficits at the time of the functional experiments.

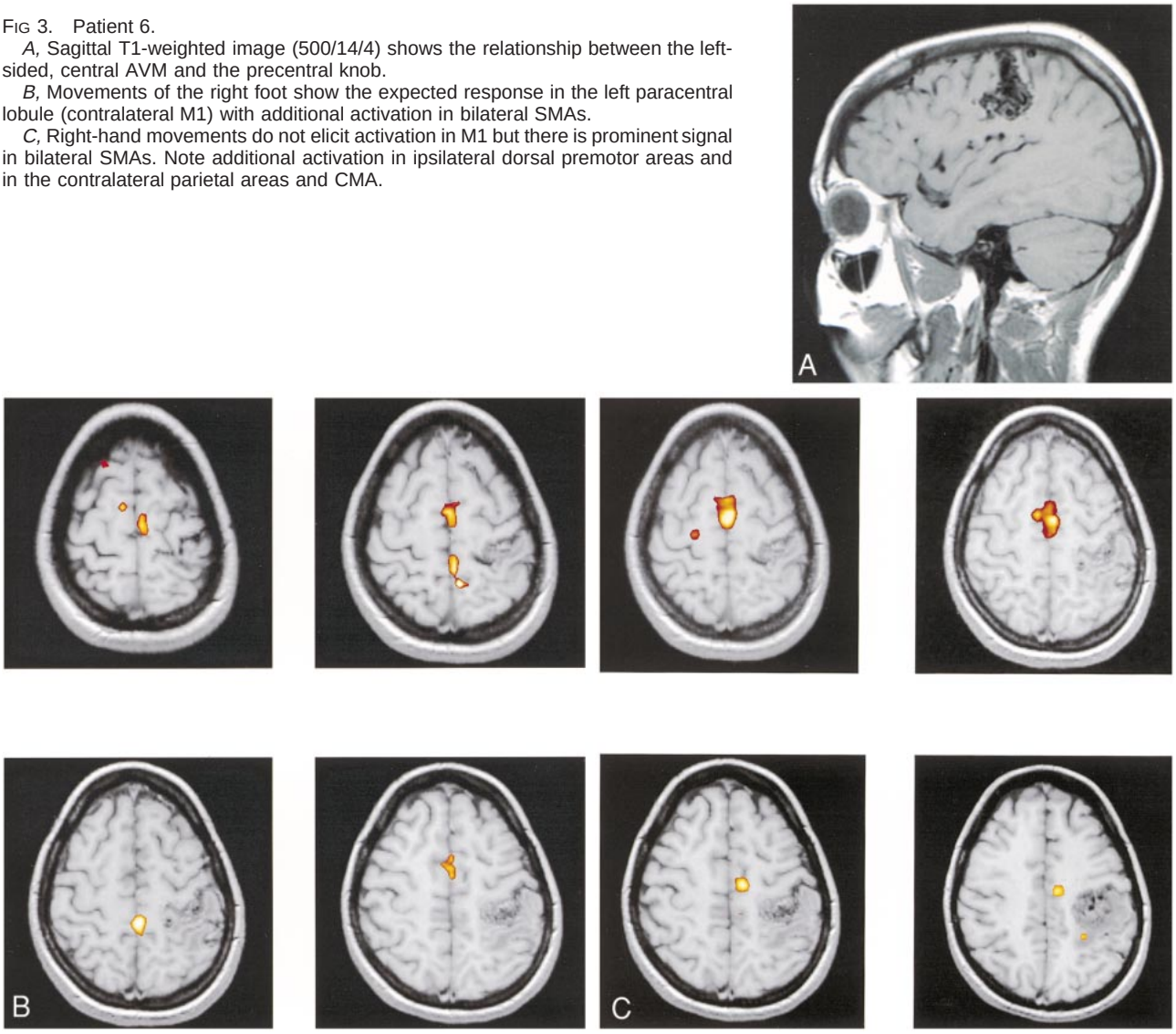

FIG 3. Patient 6.

A, Sagittal T1-weighted image (500/14/4) shows the relationship between the left-sided, central AVM and the precentral knob.

B, Movements of the right foot show the expected response in the left paracentral lobule (contralateral M1) with additional activation in bilateral SMAs.

C, Right-hand movements do not elicit activation in M1 but there is prominent signal in bilateral SMAs. Note additional activation in ipsilateral dorsal premotor areas and in the contralateral parietal areas and CMA.

In mature macaque monkeys, the use of retrogradely transported fluorescent tracers has revealed at least nine distinctive corticospinal neuron populations, originating in the frontal (including M1, SMA, and premotor areas), cingulate, insular, and parietal cortex (20, 21). They all have access to the intermediate zone and/or to the dorsal and ventral horns of the spinal cord, including the motoneurons (20, 21). It has thus been proposed that the cortical generation and control of movements at the cortical level are mediated by parallel outputs from the nonprimary as well as from the primary motor cortex (21). As a consequence, several cortical neuron populations have the potential to influence the control of voluntary movements, independent of the M1 proper (21).

Considerable experimental evidence suggests that the recovery of function after CNS damage depends on the maturity of the brain at the moment the damage is incurred (22–27). Recovery of function is generally greater when brain damage occurs early in life rather than in adulthood. These observations suggest that remaining areas of the brain are able to take over behavioral functions that normally occur in the damaged areas, and that the brain possesses a greater ability to compensate in its immature than in its mature state (22–27).

Cortical organization in the present study showed three patterns: 1) functional displacement within the contralateral M1, 2) activation originating in the unaffected M1 ipsilateral to the moving limb, and 3) function taken over from nonprimary motor areas. These results are in accordance with findings of large-scale reorganization observed in primate studies. Rouiller et al (25) demonstrated that both the stage of development at the time of an induced lesion and the extent of the lesion can play a major role in triggering different plastic changes contributing to the preservation of motor functions. Depending on the maturity of corticospinal projections and the degree of invasion of targets within the spinal cord, different patterns of re-

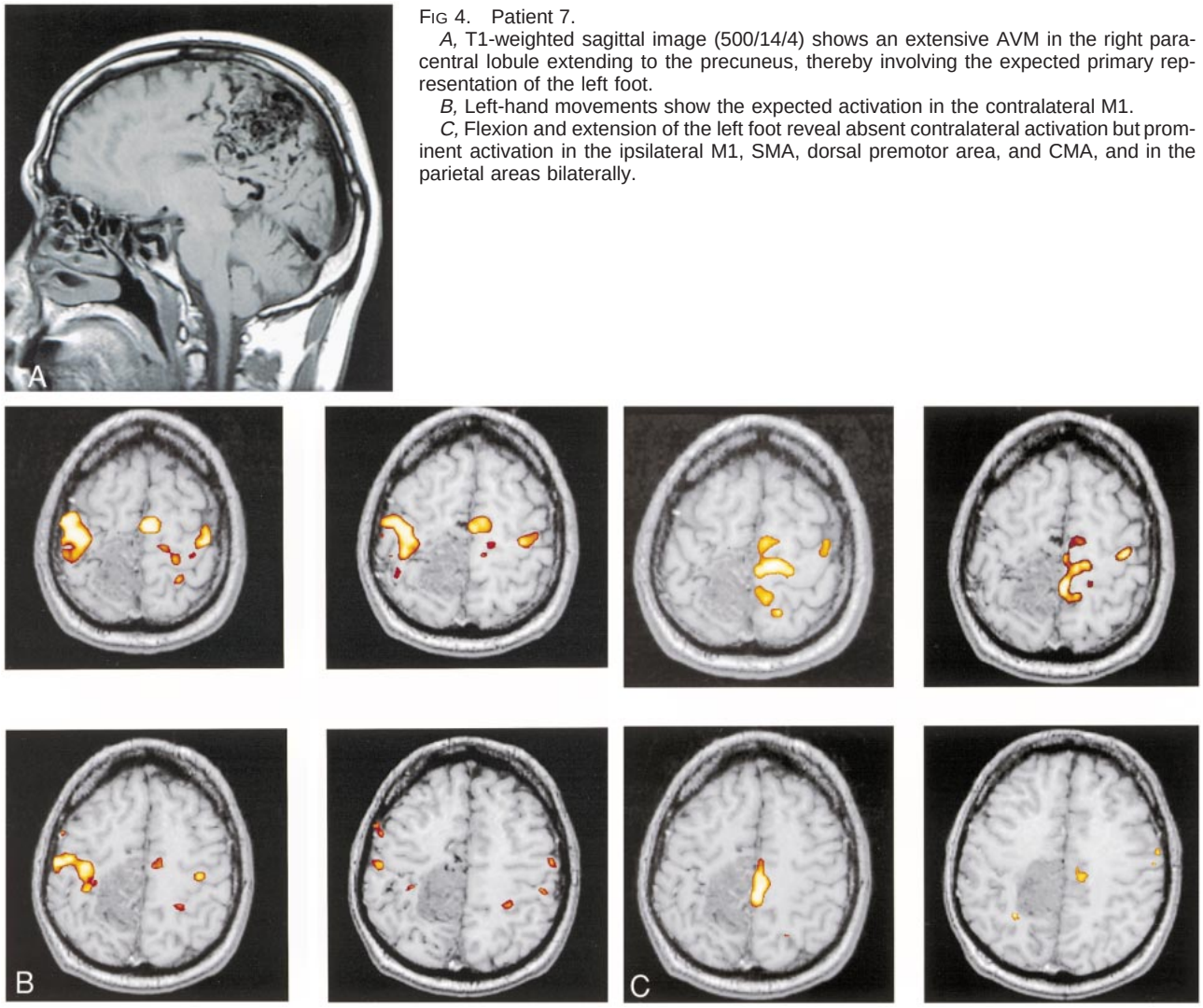

FIG 4. Patient 7.

A, T1-weighted sagittal image (500/14/4) shows an extensive AVM in the right paracentral lobule extending to the precuneus, thereby involving the expected primary representation of the left foot.

B, Left-hand movements show the expected activation in the contralateral M1.

C, Flexion and extension of the left foot reveal absent contralateral activation but prominent activation in the ipsilateral M1, SMA, dorsal premotor area, and CMA, and in the parietal areas bilaterally.

organization were observed. When lesions in M1 were induced in the mature brain, a complete new map of hand and arm representation was found in a region adjacent to the lesion. In the immature brain, in contrast, in which corticospinal projections have not yet reached their targets in the cervical cord, lesions in M1 resulted in a functional shift to the ipsilateral, intact, hemisphere.

The exact period in which brain vascular malformations occur is still controversial, and there is increasing evidence that they may develop postnatally, thereby representing a complex endothelial cell dysfunction (4, 5). Lasjaunias (5) suggests that cerebral AVMs develop at the earliest during the perinatal period and most likely during infancy. Additionally, AVMs are often followed by later microhemorrhages or hemodynamic alterations. Findings at neurosurgical removal of AVMs have shown a high rate of small, clinically undetected, chronic hemorrhages (4). Among our nine cases, it is probable that small hemorrhagic or ischemic events in areas involved in motor control had taken place. In particular, the episodes of contralateral hemiparesis (patients 2 and 9) or the earlier seizure episodes (patients 1, 4, 5, and 6) may represent small recurrent hemorrhages.

The reorganization patterns may reflect possible differences in the genesis of the brain AVMs, both in terms of the time of their formation as well as their natural history during subsequent stages of life. Absolute proof as to the exact time of formation of the AVMs investigated in this study would have required early (postnatal or early childhood) imaging studies, which, unfortunately, were not available. The same is true for most AVMs, as, usually, they are brought to medical attention only after they become symptomatic. Therefore, the time of their development remains speculative.

In two of three patients in whom the M1 area for foot representation was involved, activation was detected ipsilaterally, whereas this was the case only in one of six patients with lesions in the M1 area for hand representation. The differences in the extent of cortical representation and the complexity of movements performed by these two body parts may play a significant role in cortical reorganiza-

tion, in addition to the effect of the timing of lesion development. In any case, the number of patients in our study, particularly those with AVMs involving the M1 foot area, is too small to draw significant conclusions.

To a certain degree, our observations resemble those found in imaging studies in patients with tumors occupying the motor cortex. These patients showed large-scale reorganization that was not only confined to the somatotopic body representation areas but that also extended to cortical areas with common output territories (28, 29). The aforementioned pathophysiology of brain AVMs, which undergo a continuous and dynamic evolution, as well as the evidence that AVMs develop at various times after birth, even after infancy, may well account for similarities in activation patterns.

In cerebral AVMs, several mechanisms, including steal effect, decreased perfusion due to associated arterial stenoses, and venous hypertension, are known to influence brain function not only adjacent to but also remote from the area of disease (2–4, 6–9, 11–14, 30, 31). Despite the variable hemodynamic delays implemented in our postprocessing studies, which were effected by the use of functional MR imaging to detect neuronal activity, we still make the assumption that BOLD signal does occur in regions affected by AVMs. However, it is possible that the hemodynamic perturbations in AVMs may impede the BOLD signal, leaving nervous activation hypothetically undetected. This may have been the case in patients 6 and 9, who both had symptoms affecting the expected, contralateral, body limbs. It remains unclear whether the lack of activation of M1 bilaterally was due to hemodynamically induced abolition of the BOLD signal or to its real absence because of reorganization of brain function. Until now, the interfering hemodynamic effects of AVMs with the functional MR imaging signal resulting from BOLD contrast have not been determined (7).

In the present investigation, no BOLD signal could be measured within the nidus of the AVMs. This result was also obtained when reprocessing the data with different hemodynamic delays and with different signal rise times, and when visually inspecting the plotted time courses of voxels in the nidus. Preliminary studies and case reports using different functional imaging techniques are in disagreement with respect to the presence or absence of significant activation within the nidus (6–14, 31, 32). The nidus represents the area of the entire AVM angioarchitecture that is interposed between the distal segments of feeding arteries and the emerging proximal segments of draining veins, where arteriovenous shunting occurs. As revealed by histopathologic findings, the nidus excludes intervening brain, whereas feeding and draining vessels are separated by brain parenchyma (33). Therefore, shunted blood within the nidus should not take part in metabolic changes occurring during neuronal activity, including oxygen consumption. Considering that the origin of the functional MR imaging signal is BOLD, activation should not be measurable within the nidus of an AVM. The conflicting results in previous reports may derive from the difficulty in distinguishing the exact border of the nidus from adjacent complex and variably dilated vessels on MR images. Intervening brain between distal feeding and proximal draining vessels could be mistaken for intranidal activation. Caution should also be used when including so-called diffuse cortical AVMs in functional imaging studies. In these lesions, a nidus, in the strictest sense, cannot be identified, and only slightly dilated vessels are commonly intermingled with normal brain tissue (2–4). This type of lesion should not be considered a true AVM, as it most probably corresponds to a proliferative type of angiopathy (2–4).

Conclusion

AVMs can serve as a model by which to analyze cortical reorganization in the developing human brain. In AVMs involving the M1 cortex, specific activation patterns extend not only to primary but also to nonprimary motor areas. These reorganization phenomena cannot be accounted for by structural displacement only. Distortion of the anatomy caused by the AVMs does not influence the location of the reorganized cortex. Since, until now, no particular type of reorganization pattern could be predicted, this study emphasizes the importance of considering individual differences in studies of cortical plasticity.

References

1. Kaplan HA, Aronson SM, Browder EJ. **Vascular malformations of the brain: an anatomical study.** *J Neurosurg* 1961;18:630–635
2. Berenstein A, Lasjaunias P. **Classification of brain arteriovenous malformations.** In: *Surgical Neuroangiography*. Berlin: Springer; 1991;4:1–88
3. Valavanis A. **The role of angiography in the evaluation of cerebral vascular malformations.** *Neuroimaging Clin N Am* 1996; 6:679–704
4. Valavanis A, Yasargil MG. **The endovascular treatment of brain arteriovenous malformations.** In: *Advances and Technical Standards in Neurosurgery.* Berlin: Springer;1998;24:131–214
5. Lasjaunias P. **Vascular remodelling and the congenital nature of arteriovenous shunts.** In: *Vascular Diseases in Neonates, Infants and Children.* Berlin: Springer;1997;53–65
6. Latchaw RE, Hu X, Ugurbil K, Hall WA, Madison MT, Heros RC. **Functional magnetic resonance imaging as a management tool for cerebral arteriovenous malformations.** *Neurosurgery* 1995;37:619–625
7. Maldjian J, Atlas SW, Howard RS, et al. **Functional magnetic resonance imaging of regional brain activity in patients with intracerebral arteriovenous malformations before surgical or endovascular therapy.** *J Neurosurg* 1996;84:477–483
8. Schlosser MJ, McCarthy G, Fulbright RK, Gore JC, Awad IA. **Cerebral vascular malformations adjacent to sensorimotor and visual cortex: functional magnetic resonance imaging studies before and after therapeutic intervention.** *Stroke* 1997; 28:1130–1137
9. Thulborn KR, Davis D, Erb P, Strojwas M, Sweeney JA. **Clinical fMRI: implementation and experience.** *Neuroimage* 1996;4: 101–107
10. Turski PA, Cordes D, Mock B, et al. **Basic concepts of functional arteriovenous MR imaging malformations.** *Neuroimaging Clin N Am* 1998;8:371–381

11. Lehericy S, Biondi A, Sourour N, et al. **Language mapping in patients with brain arteriovenous malformations: influence of hemodynamic changes on BOLD signal (abstr).** *Neuroimage* 1999;9:S678
12. Lazar RM, Marshall RS, Pile-Spellman J, et al. **Anterior translocation of language in patients with left cerebral arteriovenous malformation.** *Neurology* 1997;49:802–808
13. Marshall RS, Hacein-Bey L, Young WL, et al. **Functional reorganization induced by endovascular embolization of a cerebral AVM.** *Hum Brain Map* 1996;4:168–173
14. Leblanc R, Meyer E, Zatorre R, Tampieri D, Evans A. **Functional PET scanning in the preoperative assessment of cerebral arteriovenous malformations.** *Stereotact Funct Neurosurg* 1995; 65:60–64
15. Yousry TA, Schmid UD, Alkadhi H, et al. **Localization of the motor hand area to a knob on the precentral gyrus: a new landmark.** *Brain* 1997;120:141–157
16. Rao SM, Binder JR, Hammeke TA, et al. **Somatotopic mapping of the human primary motor cortex with functional magnetic resonance imaging.** *Neurology* 1995;45:919–924
17. Woods RP, Grafton ST, Holmes CJ, et al. **Automated image registration, I: general methods and intrasubject, intramodality validation.** *J Comput Assist Tomogr* 1998;22:139–152
18. Bandettini PA, Jesmanowica A, Wong EC, Hyde JS. **Processing strategies for time-course data sets in functional MRI of the human brain.** *Magn Reson Med* 1993;30:161–173
19. Press WH, Teukolsky SA, Vetterling WT, Flannery BP. ***Numerical Recipes in C: The Art of Scientific Computing.*** 2nd ed. New York: Cambridge University Press;1992;639–645
20. Galea MP, Darian-Smith I. **Multiple corticospinal neuron populations in the macaque monkey are specified by their unique cortical origins, spinal terminations, and connections.** *Cereb Cortex* 1994;4:166–194
21. Dum RP, Strick PL. **The origin of corticospinal projections from the premotor areas in the frontal lobe.** *J Neurosci* 1991; 11:667–689
22. Carr LJ. **Development and reorganization of descending motor pathways in children with hemiplegic cerebral palsy.** *Acta Paediatr Suppl* 1996;416:53–57
23. Kennard MA. **Cortical reorganization of motor function: studies on a series of monkeys of various ages from infancy to maturity.** *Arch Neurol Psychiatry* 1942;48:227–240
24. Passingham RE, Perry VH, Wilkinson F. **The long-term effects of removal of sensorimotor cortex in infant and adult monkeys.** *Brain* 1983;106:675–705
25. Rouiller EM, Yu XH, Moret V, Tempini A, Wiesendanger M, Liang F. **Dexterity in adult monkeys following early lesion of the motor cortical hand area: the role of cortex adjacent to the lesion.** *Eur J Neurosci* 1998;10:729–740
26. Benecke R, Meyer BU, Freund HJ. **Reorganisation of descending motor pathways in patients after hemispherectomy and severe hemispheric lesions demonstrated by magnetic brain stimulation.** *Exp Brain Res* 1991;83:419–426
27. Spear PD. **Plasticity following neonatal visual cortex damage in cats.** *Can J Physiol Pharmacol* 1995;73:1389–1397
28. Seitz RJ, Huang Y, Knorr U, Tellmann L, Herzog H, Freund H-J. **Large-scale plasticity of the human motor cortex.** *Neuroreport* 1995;6:742–744
29. Fandino J, Kollias SS, Wieser HG, Valavanis A, Yonekawa Y. **Intraoperative validation of functional magnetic resonance imaging and cortical reorganization patterns in patients with brain tumors involving the primary motor cortex.** *J Neurosurg* 1999;91:238–250
30. Yasargil MG. **Hemodynamics.** In: *Microneurosurgery.* Stuttgart: Thieme;1987; IIIA:213–239
31. Grafton ST, Martin NA, Mazziotta JC, Woods RP, Vinuela F, Phelps ME. **Localization of motor areas adjacent to arteriovenous malformations: a positron emission tomographic study.** *J Neuroimag* 1994;4:97–103
32. Leblanc R, Meyer E. **Functional PET scanning in the assessment of cerebral arteriovenous malformations: case report.** *J Neurosurg* 1990;73:615–619
33. Burger PC, Scheithauer BW. **Vascular tumors and tumor-like lesions.** In: *Tumors of the Central Nervous System.* Washington, DC: Armed Forces Institute of Pathology;1994;287–299

Appendix

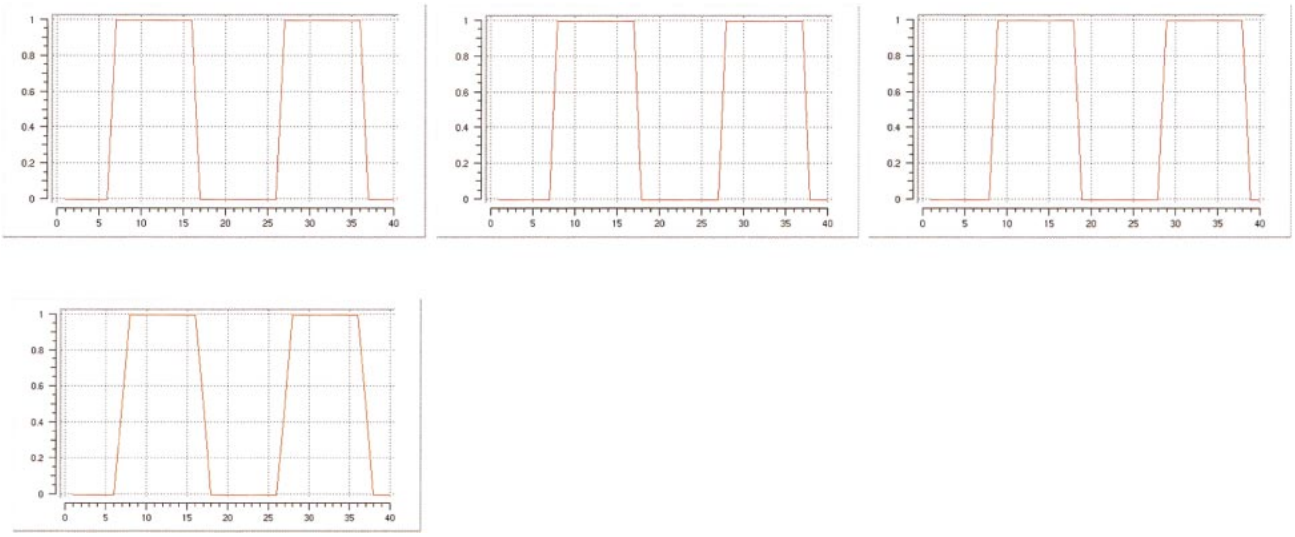

FIG A1. Plotted signal models of the boxcar functions with different time delays (one, two, and three TRs; *upper row*), and the trapezoidal function with a one-TR delay and a rise time of two TRs (*lower image*).

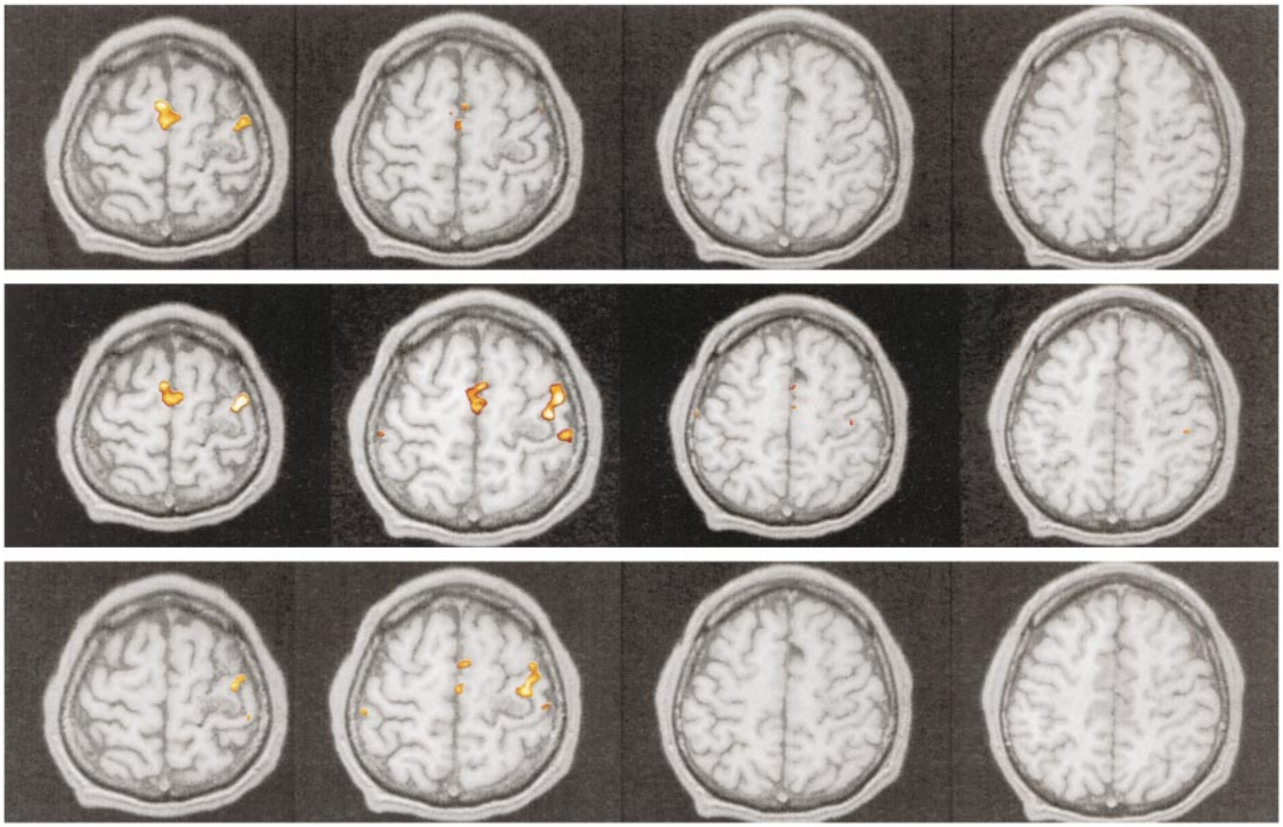

FIG A2. Patient 1. Reprocessed functional MR imaging experiment using a boxcar function with delays of one TR (*upper row*), two TRs (*middle row*), and three TRs (*lower row*).

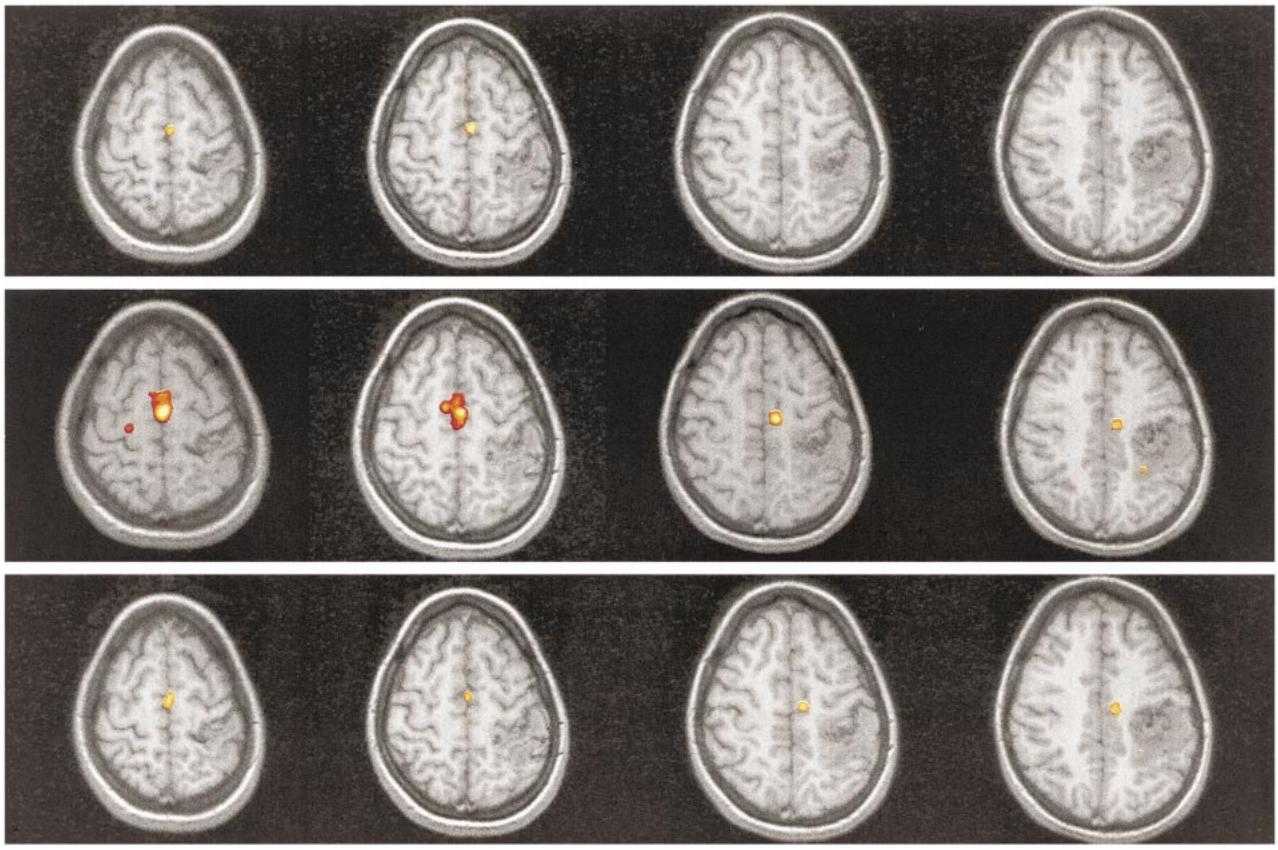

FIG A3. Patient 6. Reprocessed functional MR imaging experiment using a boxcar function with delays of one TR (*upper row*), two TRs (*middle row*), and three TRs (*lower row*).

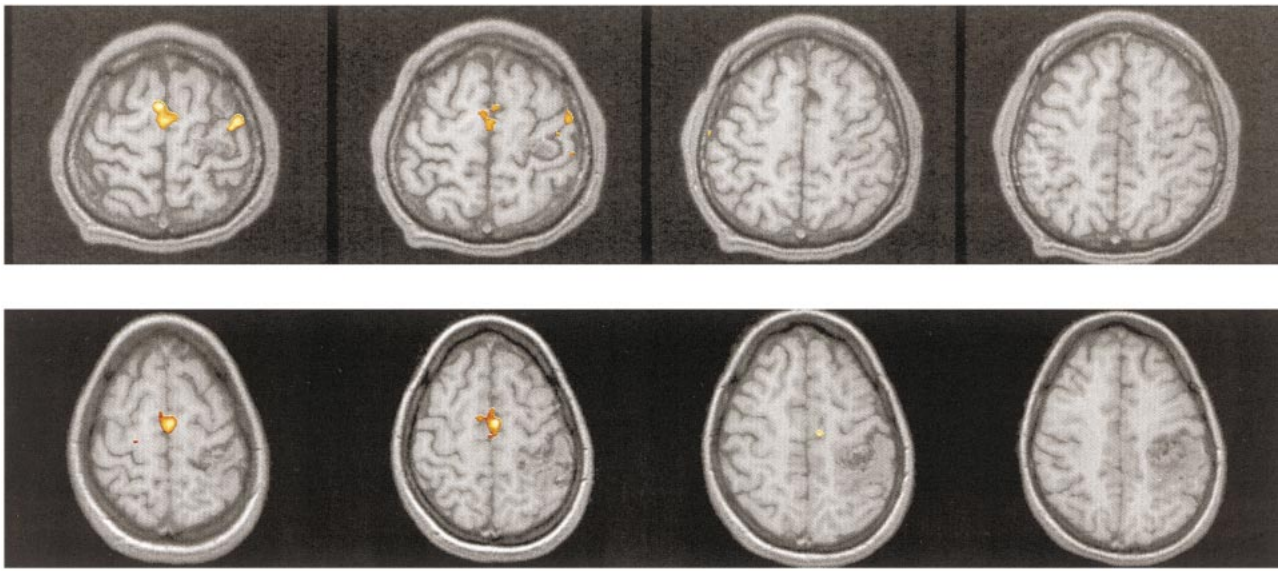

FIG A4. Reprocessed functional MR imaging experiment using a trapezoidal function with a delay of one TR and a rise time of two TRs in patients 1 (*upper row*) and 6 (*lower row*).